



Effect of indium doping on (CdZn)Se composite thin films

P.A. Chate^{a,*}, P.P. Hankare^b, D.J. Sathe^c

^a Department of Chemistry, J.S.M. College, J.S.M. Road, Alibag, M.S. 402 201, India

^b Solid State Research Laboratory, Dept. of Chemistry, Shivaji University, Kolhapur, M.S., India

^c Dept. of Chemistry, KIT's Engineering College, Kolhapur, M.S., India

ARTICLE INFO

Article history:

Received 11 May 2010

Received in revised form 7 June 2010

Accepted 10 June 2010

Available online 18 June 2010

Keywords:

Thin films

Doping

Chemical bath deposition

Film characterization

Optical properties

ABSTRACT

Cd_{0.9}Zn_{0.1}Se:In thin films with a variable composition (0–1.0 mol% indium) have been grown on a non-conducting glass substrate by chemical bath deposition method. The effect of doping has been investigated. The color of a film was found to be darkening with increase in the concentration of indium. X-ray diffraction, optical absorption, electrical and thermoelectrical techniques were used to characterize the films. The X-ray diffraction study indicates the crystalline nature in single cubic phase over whole range of composition. Analysis of absorption spectra gave direct type of band gap, the magnitude of which varies non-linearly as the indium content in the film increases. The dc electrical conductivity increases up to 0.1 mol%. The promising features observed are the enhancement in crystallinity, grain size, electrical conductivity and decrease in band gap, up to 0.1 mol%.

© 2010 Elsevier B.V. All rights reserved.

1. Introduction

In the modern days, binary as well as pseudo-binary semiconductors have been attracting much interest in photovoltaic. Because of their electronic and optical properties, Cd_{1-x}Zn_xSe materials are applied in radiation detectors and laser screen materials in projection color TV [1–3]. Cd_{1-x}Zn_xSe is one of the important materials in electroluminescent, photoconductive and photovoltaic applications [4–7]. This system facilitates the development of several new electronic devices such as light emitting diodes, photodetectors, blue green lasers [8]. Thin films of (CdZn)Se have been prepared by molecular beam epitaxy, electron beam evaporation, electrodeposition, etc. [9–11]. Chemical bath deposition method is an alternative, low cost method which can operate at low processing temperature and can give large deposition area [12]. The electronic and optical properties of semiconductors are strongly influenced by the doping process, which provides the basis for tailoring the desired carrier concentration and, consequently, the absorption, emission and transport properties as well. When the density of n-type or p-type doping becomes sufficiently high, the impurity merges with conduction and valence band and causes the formation of band tail and band gap shrinkage [13–15]. In photoelectrochemical cells, one of the reason in the loss in conversion efficiency is due to higher resistivity of the photoelec-

trode material. An efficient way to decrease the resistivity and to improve the properties of semiconducting material is to dope with a suitable impurity like copper, silver, aluminum and indium. The dopant has shown to enhance properties in number of host lattices [16–20]. In Cd_{1-x}Zn_xSe system, a Cd_{0.9}Zn_{0.1}Se thin film has the lowest band gap, activation energy as well as resistivity [21]. To decrease the resistivity the material is doped with suitable dopant like indium.

This paper deals with successful room temperature deposition of Cd_{0.9}Zn_{0.1}Se:In thin films by chemical bath deposition. The structural, morphological, optical, thermoelectrical and electrical properties are studied with respect to doping concentration.

2. Experimental procedure

All the chemicals used were of AR grade. Sodium selenosulphate was prepared by following the method reported earlier [22]. The deposition of a typical Cd_{0.9}Zn_{0.1}Se:In thin films was made in a reactive solution containing 9 mL (0.2 M) cadmium sulphate octahydrate, 1 mL (0.2 M) zinc sulphate, 2.5 mL (1 M) tartaric acid, 25 mL (2%) hydrazine hydrate and 10 mL (0.2 M) sodium selenosulphate. The varying concentration of indium from 0.01 to 1.0 mol% was used. The total volume of the reaction mixture was made to 150 mL by adding double distilled water. The beaker containing reactive solution was transferred to ice bath of 278 K. The pH was found to be 12.00 ± 0.05. Four-glass substrate was kept vertically in a reaction mixture and rotated with a speed of 50 ± 2 rpm. The temperature of the solution was allowed to rise slowly to room temperature. The substrates were removed from the beaker after 240 min. After the deposition, the substrates were taken out of the bath, rinsed with distilled water, dried in air and kept in a desiccator.

* Corresponding author. Tel.: +91 0231 2693501.

E-mail addresses: pachate04@rediffmail.com, pachate09@rediffmail.com (P.A. Chate).

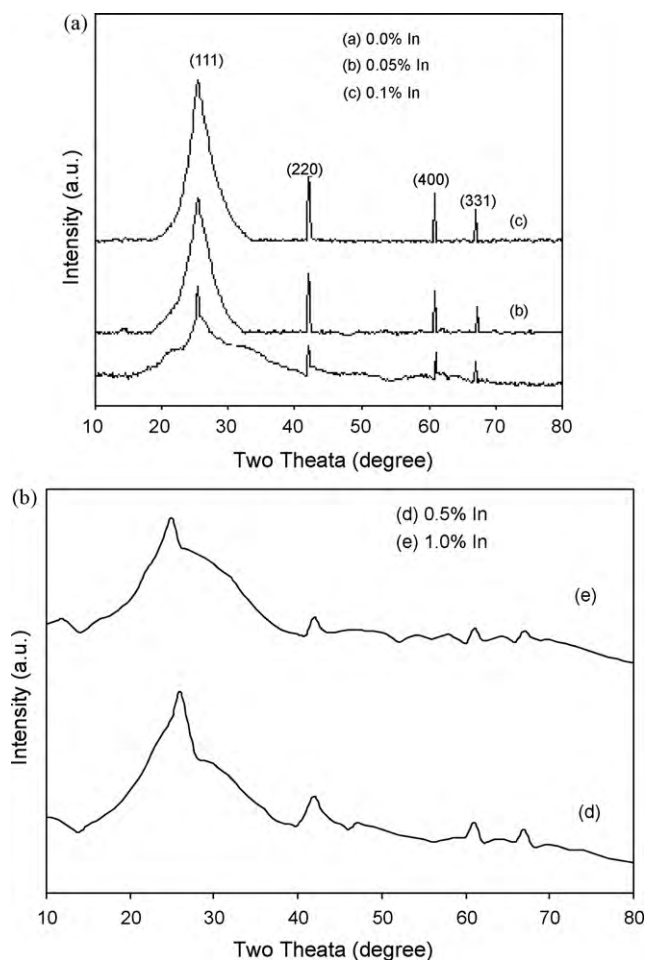


Fig. 1. XRD pattern of $\text{Cd}_{0.9}\text{Zn}_{0.1}\text{Se}:\text{In}$ chemically deposited typical thin film. (a) Doping concentration 0.0, 0.05, 0.1 mol% indium and (b) doping concentration 0.5, 1.0 mol% indium.

3. Results and discussions

3.1. Physical properties

Indium doped $\text{Cd}_{0.9}\text{Zn}_{0.1}\text{Se}$ thin films were found to be uniform and well adherent to the substrate. The color of the films was found to be darkening with increase in the concentration of In. The layer thickness of the film was estimated by the weight difference method. The film thickness increases from 0.72 to 0.80 μm as doping concentration increases up to 0.1 mol%, thereafter it decreases. This is due to substitutional inclusion of indium ions in the interstitial position of lattice or in cationic vacancies already present in the host. At higher doping concentration, the impurity atom may be occupying interstitial sites causing an impurity scattering and thereby preventing further growth of the film [23].

3.2. XRD studies

$\text{Cd}_{0.9}\text{Zn}_{0.1}\text{Se}:\text{In}$ films were characterized by using a Philips PW-1710 diffractometer in 2θ range from 10° to 80° using $\text{Cu K}\alpha_1$ radiation ($\lambda = 1.54056 \text{ \AA}$). The chalcogenides of Cd as well as Zn normally show the duality in their crystal structure. They can be formed with either sphalerite (cubic, zinc blend type) or wurtzite (hexagonal type) structure [3,24]. The X-ray diffraction (XRD) spectra of $\text{Cd}_{0.9}\text{Zn}_{0.1}\text{Se}:\text{In}$ thin films deposited on glass substrate are shown in Fig. 1. The spectra for pure CdSe (JCPDF card no. 19-191, JCPDS

card no. 8-459) and pure ZnSe (JCPDF card no. 1463) were used for identification purpose. The XRD pattern shows a large number of peaks indicating that the films are crystalline in nature. The analysis of spectrum indicated that all the films have cubic structure (sphalerite) in the whole range of compositions studied. The other phases of CdSe and ZnSe (hexagonal) have not been observed. The analysis of XRD patterns in terms of hkl planes, interplanar distances, cell size, lattice parameters have been done by considering sphalerite structure and is displayed in Table 1.

All films show (1 1 1) most intense peak reflection observed that for $\text{Cd}_{0.9}\text{Zn}_{0.1}\text{Se}:\text{In}$ thin films were originating from (1 1 1) plane. Along with (1 1 1) plane, (2 2 0), (4 0 0), (3 3 1) planes were observed. The peak intensity and crystallinity of the films were found to increase with In doping concentration up to 0.1 mol%. For higher In doping concentration, the materials tend to decrease crystallinity. This behavior could be explained on the basis of surface adsorption of indium atoms over a growing film preventing further growth of the microcrystals. Tl, Ag, Sb, have obtained the similar type of results on doping in host structure [25–27]. All the In-doped films show the strongest peak occurs approximately at the same 'd' value with a little modification of peak width and intensity. The constancy in the 'd' value of prominent peaks shows that due to indium doping, the lattice of host material is neither shrinking nor expanding. Thus indium ion doping does not change the cell symmetry. The lattice parameter was determined by using the formula:

$$a = d(h^2 + k^2 + l^2)^{1/2} \quad (1.1)$$

It is found that up to 0.1 mol%, the lattice parameter increases smoothly from 6.0687 to 6.0829 \AA , thereafter decreases up to 6.0644 \AA for 1.0 mol% indium concentration. The average crystallite size was calculated by resolving the highest intensity peak (1 1 1). The average crystallite size was determined by using Scherrer's formula. Up to 0.1 mol% In, the particle size increases from 190 to 230 \AA , thereafter decreases up to 183 \AA for 1.0 mol% In concentration.

3.3. Optical studies

The optical absorption measurement was made by using a Hitachi-330 (Japan) UV-VIS-NIR double beam spectrophotometer in the wavelength range from 350 to 750 nm. The absorption spectra are used to calculate absorption coefficient, optical band gap and type of transition. The absorption spectra of representative indium doped films are shown in Fig. 2. For all the compositions, the value of absorption coefficient is high. The data were systematically studied in the vicinity of the absorption edge on the basis of three-dimensional model. The simplest form of equations obeyed near and above absorption edge is [28]:

$$\alpha h\nu = A(h\nu - E_g)^n \quad (1.2)$$

where the symbols have their usual meaning.

Up to 0.1 mol%, the absorption edge shifted towards higher wavelength. This is due to filling of low lying energy level by conduction electron and segregation of the impurity along the grain boundary [29]. A plot of $(\alpha h\nu)^2$ versus $h\nu$ should be a straight line whose intercept to the x-axis gives the optical band gap. The plot of $(\alpha h\nu)^2$ versus $h\nu$ is shown in Fig. 3. The linear nature of plot shows the existence of direct transition. It is observed that the band gap decreases from 1.88 to 1.78 eV as the indium concentration increases up to 0.1 mol%. Above 0.1 mol% the band gap increases up to 1.78–1.93 eV. This is due to increased amount of disorder caused by addition of indium in the host lattice [30]. The variation of band gap with concentration of indium is shown in Fig. 4. The values of band gap of different compositions are listed in Table 2.

Table 1
Crystallographic parameters of Cd_{0.9}Zn_{0.1}Se:In thin films.

Doping concentrations in Cd _{0.9} Zn _{0.1} Se (mol%)	Observed 'd' values (Å)	Std. 'd' values (Å)		hkl	Grain size (Å)	Cell parameters (Å)
		ZnSe (cubic)	CdSe (cubic)			
0.0	3.500	3.273	3.51	111	190	6.0687
	2.147	2.003	2.149	220		
	1.516	1.416	1.519	400		
	1.394	1.299	1.394	331		
0.01	3.505	3.273	3.51	111	195	6.0737
	2.148	2.003	2.149	220		
	1.517	1.416	1.519	400		
	1.395	1.299	1.394	331		
0.025	3.507	3.273	3.51	111	201	6.0752
	2.149	2.003	2.149	220		
	1.518	1.416	1.519	400		
	1.394	1.299	1.394	331		
0.05	3.508	3.273	3.51	111	211	6.0758
	2.148	2.003	2.149	220		
	1.520	1.416	1.519	400		
	1.393	1.299	1.394	331		
0.075	3.510	3.273	3.51	111	219	6.0782
	2.150	2.003	2.149	220		
	1.518	1.416	1.519	400		
	1.395	1.299	1.394	331		
0.1	3.512	3.273	3.51	111	230	6.0829
	2.151	2.003	2.149	220		
	1.520	1.416	1.519	400		
	1.396	1.299	1.394	331		
0.25	3.510	3.273	3.51	111	194	6.0785
	2.149	2.003	2.149	220		
	1.519	1.416	1.519	400		
	1.395	1.299	1.394	331		
0.5	3.507	3.273	3.51	111	190	6.0735
	2.148	2.003	2.149	220		
	1.517	1.416	1.519	400		
	1.394	1.299	1.394	331		
0.75	3.504	3.273	3.51	111	187	6.0687
	2.146	2.003	2.149	220		
	1.516	1.416	1.519	400		
	1.393	1.299	1.394	331		
1.0	3.503	3.273	3.51	111	183	6.0644
	2.145	2.003	2.149	220		
	1.514	1.416	1.519	400		
	1.392	1.299	1.394	331		

3.4. Electrical conductivity and thermoelectrical studies

The electrical conductivity of In-doped Cd_{0.9}Zn_{0.1}Se thin film on non-conducting glass substrate was determined by using a 'dc' two-probe method in the temperature range 300–525 K. The electrical

conductivity at room temperature increases as the indium concentration increases up to 0.1 mol% and thereafter value decreases for higher concentration. Up to 0.1 mol% incorporation of In at their lattice host resulted in decrease in boundary potential and improvement in crystallite size, which results in the increase of

Table 2
Optical and electrical parameters of Cd_{0.9}Zn_{0.1}Se:In thin films.

Sr. no.	Doping concentrations in Cd _{0.9} Zn _{0.1} Se (mol%)	Band gap (eV)	Specific resistance (Ω cm)		Thickness (μm)	Activation energy (eV)
			At 300 K	At 525 K		
1	0.0	1.90	7.98 × 10 ⁶	1.54 × 10 ³	0.72	0.685
2	0.01	1.88	7.10 × 10 ⁶	1.45 × 10 ³	0.74	0.671
3	0.025	1.85	5.46 × 10 ⁶	1.37 × 10 ³	0.75	0.655
4	0.05	1.82	3.60 × 10 ⁶	1.29 × 10 ³	0.77	0.642
5	0.075	1.80	2.59 × 10 ⁶	1.21 × 10 ³	0.78	0.626
6	0.1	1.78	2.27 × 10 ⁶	1.14 × 10 ³	0.80	0.608
7	0.25	1.81	3.15 × 10 ⁶	1.24 × 10 ³	0.75	0.627
8	0.5	1.85	5.68 × 10 ⁶	1.42 × 10 ³	0.73	0.649
9	0.75	1.89	7.60 × 10 ⁶	1.49 × 10 ³	0.71	0.673
10	1.0	1.93	8.59 × 10 ⁶	1.91 × 10 ³	0.69	0.698

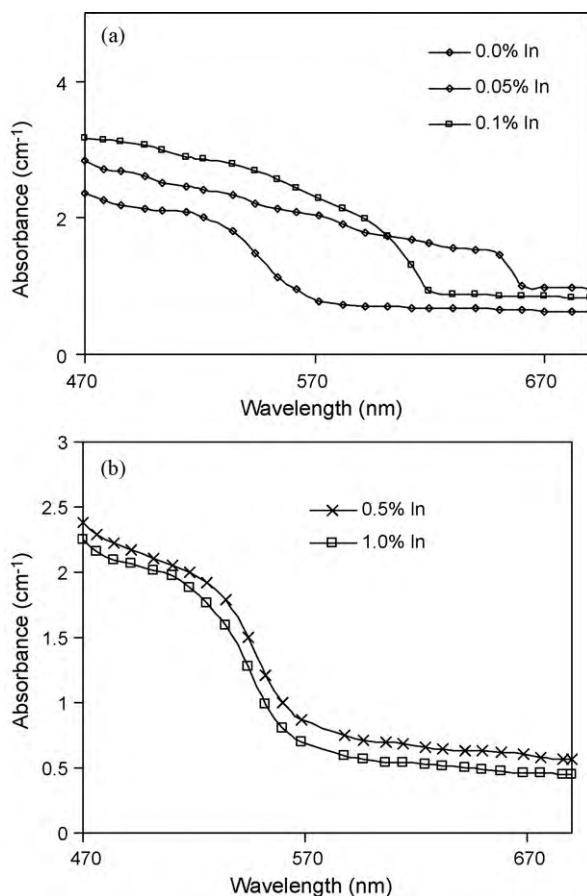


Fig. 2. Absorption spectra for Cd_{0.9}Zn_{0.1}Se:In thin films. (a) Doping concentration 0.0, 0.05, 0.1 mol% indium and (b) doping concentration 0.5, 1.0 mol% indium.

carrier concentration as well as mobility [31]. As the size of In³⁺ ion is less than Cd²⁺ ion, the incorporation could cause a scattering process thereby reducing the mobility [32,33]. Above 0.1 mol% the conductivity decreases, as more and more distortion is observed in the lattice structure, which results in increase in grain boundary scattering, thereby reducing the carrier mobility [34,35]. The electrical conductivity variation with temperature during heating and cooling cycles was found to be different and this shows that the 'as deposited' films undergo an irreversible change due to annealing out of non-equilibrium defects during first heating. The activation energy is calculated using exponential form of Arrhenius equation:

$$\sigma = \sigma_0 \exp\left(-\frac{E_a}{KT}\right) \quad (1.3)$$

where the terms have usual meaning.

The variation of log (conductivity) versus inverse absolute temperature for the cooling curve is shown in Fig. 5. The activation energy is found to decrease up to 0.1 mol% and increase for higher concentration. The value of activation energy as well as specific resistance at 300 and 525 K is listed in Table 2.

In thermoelectric power measurements, the open circuit thermovoltage generated by the samples, when a temperature gradient is applied across the 2 cm length of the sample, was measured. From the sign of the terminal connected to the cold end of the sample, one can deduce the sign of the predominant charge carriers in the case of Cd_{0.9}Zn_{0.1}Se:In thin films, the negative terminal was connected to the cold end, therefore, the film shows n-type conductivity.

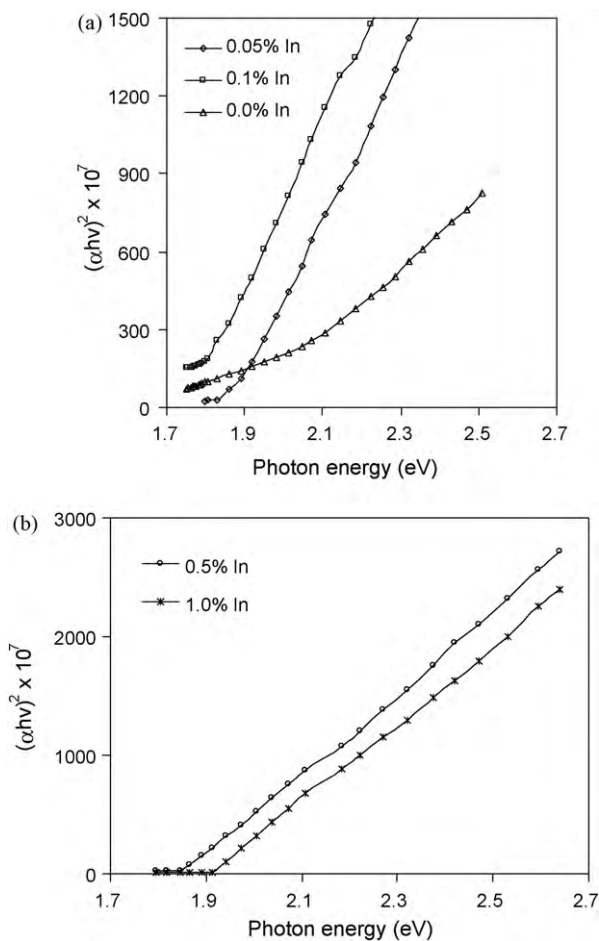


Fig. 3. Determination of band gap for Cd_{0.9}Zn_{0.1}Se:In thin films. (a) Doping concentration 0.0, 0.1 mol% indium and (b) doping concentration 0.5, 1.0 mol% indium.

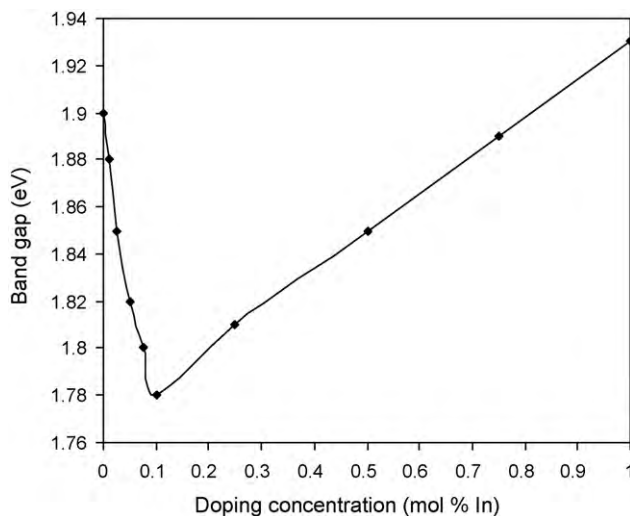


Fig. 4. Variation of band gap with doping concentration for Cd_{0.9}Zn_{0.1}Se:In thin films.

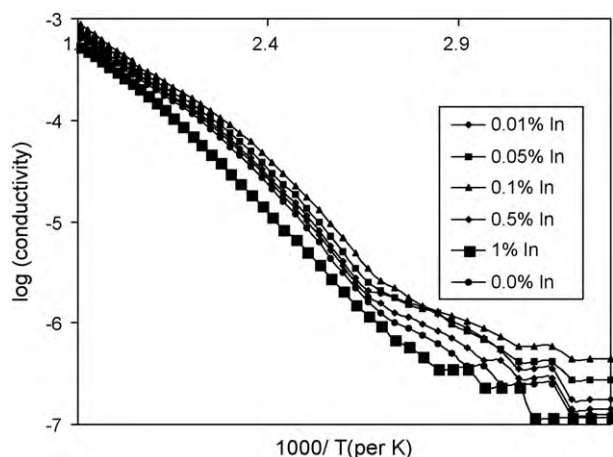


Fig. 5. Plot of log (conductivity) versus inverse of absolute temperature for $\text{Cd}_{0.9}\text{Zn}_{0.1}\text{Se}:\text{In}$ thin films.

4. Conclusion

- (1) Indium doped $\text{Cd}_{0.9}\text{Zn}_{0.1}\text{Se}$ thin films can be deposited by using chemical bath deposition method. The indium donor atoms were found to dissolve substitutionally in the lattice of $\text{Cd}_{0.9}\text{Zn}_{0.1}\text{Se}$ up to a certain range of doping concentration.
- (2) The films grow highly oriented in the cubic phase. No appreciable shifting of peaks was observed. The crystallinity and particle size were found to increase with indium concentration up to 0.1 mol% whereas for higher values of indium, the material decreases crystallinity.
- (3) The absorption study shows the presence of direct band gap. The band gap decreases from 1.90 to 1.78 eV as the doping concentration increases from 0 to 0.1 mol% whereas for higher values of indium, the band gap increases.
- (4) The specific conductance at room temperature for all the films was found to be in the order of $10^{-6} (\Omega \text{ cm})^{-1}$. The electrical conductivity study indicated the presence of only one conduction mechanism. The conductivity increases while activation energy decreases up to 0.1 mol%, thereafter it decreases.

References

- [1] K.Y. Rajpure, S.M. Bhamane, C.D. Lokhande, C.H. Bhosale, *Ind. J. Pure Appl. Phys.* 37 (1999) 413.
- [2] J.-C. Jan, S.-Y. Kuo, S.-B. Yin, W.-F. Hsieh, *Chin. J. Phys.* 39 (2001) 90.
- [3] R.B. Kale, S.D. Sartale, B.K. Chougale, C.D. Lokhande, *Semicond. Sci. Technol.* 19 (2004) 980.
- [4] D.S. Suttrave, G.S. Shahane, V.B. Patil, L.P. Deshmukh, *Mater. Chem. Phys.* 65 (2000) 298.
- [5] T.M. Razykov, *Thin Solid Films* 164 (1988) 301.
- [6] A. Burger, M. Roth, *J. Cryst. Growth* 70 (1989) 867.
- [7] A.S. Nasibov, Y.V. Korostelin, L.G. Suslina, D.L. Fedorav, L.S. Markov, *Solid State Commun.* 71 (1989) 867.
- [8] N. Samrath, H. Luo, J.K. Furdyna, S.B. Quadri, Y.R. Lee, R.G. Alonso, E.K. Suh, A.K. Ramdas, N. Ofsuka, *Surf. Sci.* 228 (1990) 226.
- [9] R.Z. Feng, S.P. Guo, *J. Mater. Sci. Lett.* 15 (1994) 1824.
- [10] R. Islam, R.R. Rao, *J. Mater. Sci. Lett.* 13 (1994) 1637.
- [11] R. Chandramohan, T. Mahalingam, J.P. Chu, P.J. Sebastian, *Sol. Energy Mater. Sol. Cells* 81 (2004) 371.
- [12] M. Ganchev, N. Stratieva, E. Tzvetkova, *J. Mater. Sci.: Mater. Electron.* 14 (2003) 847.
- [13] G. Perma, V. Capozzi, A. Minafra, M. Pallara, M. Ambrico, *Eur. Phys. J.* B32 (2003) 339.
- [14] E.O. Kane, *Phys. Rev.* 131 (1969) 79.
- [15] A. Haufe, R. Schwabe, H. Fieseler, M. Illegems, *J. Phys. C21* (1988) 2951.
- [16] L.P. Deshmukh, S.G. Holikatti, B.M. More, *Mater. Chem. Phys.* 39 (1995) 743.
- [17] S.H. Pawar, L.P. Deshmukh, *Ind. J. Pure Appl. Phys.* 22 (1884) 315.
- [18] N.R. Pavaskar, C.A. Menezes, A.B.P. Sinha, *J. Electrochem. Soc.* 124 (1977) 743.
- [19] H. Gerischer, *Electroanal. Chem.* 58 (1975) 263.
- [20] L.P. Deshmukh, A.B. Palwe, V.S. Sawant, *Sol. Energy Mater.* 20 (1990) 341.
- [21] P.P. Hankare, P.A. Chate, M.R. Asabe, S.D. Delekar, I.S. Mulla, K.M. Garadkar, *J. Mater. Sci.: Mater. Electron.* 17 (2006) 1055.
- [22] V.M. Bhuse, P.P. Hankare, K.M. Garadkar, A.S. Khomane, *Mater. Chem. Phys.* 80 (2003) 82.
- [23] S. Jatar, A.C. Rastogi, V.G. Bhide, *Pramana* 16 (1978) 477.
- [24] M. Bouroushian, Z. Loizos, N. Spyrellis, G. Maurin, *Appl. Surf. Sci.* 115 (1997) 103.
- [25] T. Suzuki, Y. Ema, T. Hayashi, *Jpn. J. Appl. Phys.* 26 (1987) 2009.
- [26] K.C. Sharma, R. Sharma, J.C. Garg, *Jpn. J. Appl. Phys.* 31 (1992) 742.
- [27] P.P. Hankare, A.D. Jadhav, V.M. Bhuse, A.S. Khomane, *Mater. Chem. Phys.* 80 (2003) 103.
- [28] J. Bardeen, F.J. Blatt, L.H. Hall, in: R. Brechepride Russel, E. Hahn (Eds.), *Proceedings of the Photoconductivity Conference*, Wiley, NY, 1975.
- [29] L.P. Deshmukh, B.M. More, S.G. Holikatti, *Bull. Mater. Sci.* 17 (1994) 455.
- [30] S. Bhushan, S. Srivastav, *Ind. J. Pure Appl. Phys.* 33 (1995) 371.
- [31] J. Rodriguez, G. Gordillo, *Sol. Energy Mater.* 19 (1989) 421.
- [32] B.D. Cullity, *Elements of X-ray Diffraction*, 2nd ed., Wesley Pub. Co.; Inc., Phillipine, 1978.
- [33] S. Chandra, in: D.S. Campbell (Ed.), *Photoelectrochemical Cells*, vol. 5, Gardon and Breach Science Publishers, New York, 1985.
- [34] L.P. Deshmukh, C.B. Rotti, G.S. Shahane, *Ind. J. Pure Appl. Phys.* 36 (1998) 322.
- [35] K. Subramanian, V. Sunder Raja, *Sol. Energy Mater. Sol. Cells* 32 (1994) 1.